Journal of Sustainable Metallurgy (2021) 7:1190–1199
https://doi.org/10.1007/s40831-021-00413-8

RESEARCH ARTICLE

Effect of B_2O_3 on the Melting Temperature and Viscosity of $CaO–SiO_2–MgO–Al_2O_3–TiO_2–Cr_2O_3$ Slag

Jing Ma[1,2] · Wei Li[1,2] · Guiqin Fu[1,2] · Miaoyong Zhu[1,2]

Received: 18 April 2021 / Accepted: 18 July 2021 / Published online: 28 July 2021

Abstract

Fluorite is widely employed as a fluxing agent in metallurgical processes, inevitably leading to severe pollution. In this study, to promote the development of sustainable metallurgy, B_2O_3 is used as a fluxing agent of $CaO–SiO_2–MgO–Al_2O_3–TiO_2–Cr_2O_3$ slag, acting as a replacement for CaF_2. The effect of B_2O_3 on the melting temperature and viscosity of $CaO–SiO_2–MgO–Al_2O_3–TiO_2–Cr_2O_3$ slag was investigated using a melting-point and melting-rate measurement instrument and a melting physical property comprehensive measurement instrument. Scanning electron microscopy was used to observe the microstructure of the precipitated phase, and X-ray diffraction was used to identify its phase composition. The results indicated that both the melting temperature and viscosity decreased with increasing B_2O_3 content. Moreover, B_2O_3 had a significant influence on the morphology of the precipitated phase, particularly for the shape and size of the precipitated particles. Accordingly, with the increase in the B_2O_3 content, the composition of the precipitated phase and the corresponding diffraction peak intensities changed. The results of this study provide a theoretical and technical basis for the comprehensive utilization of Cr-containing high-titanium melting slag.

Graphical Abstract

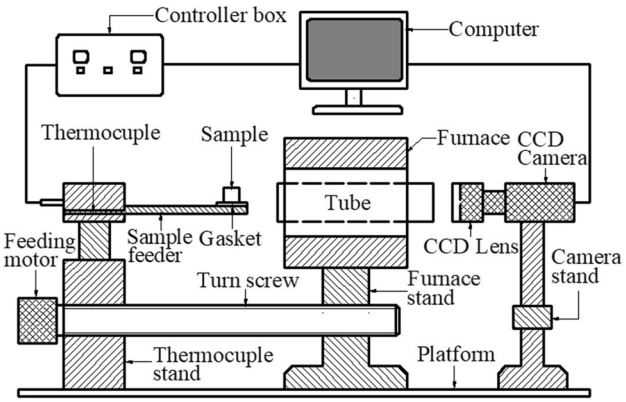

Keywords B_2O_3 · Cr-containing high-titanium melting slag · Melting temperature · Viscosity · Phase composition

Introduction

Vanadium titanomagnetite (VTM) is a multi-component mineral that contains Fe, Ti, V, and various rare metals. In addition to Fe, Ti, and V, Hongge VTM (HVTM) found in the deposits in the Panzhihua-Xichang area also has a high chromium content and is the largest VTM resource in China [1, 2]. Currently, two processes are mainly used for

The contributing editor for this article was Mansoor Barati.

✉ Wei Li
lw_neu@126.com

✉ Miaoyong Zhu
myzhu@mail.neu.edu.cn

Extended author information available on the last page of the article

the utilization of HVTM, namely, the blast furnace (BF) process and coal-based direct reduction process. However, for both the BF and coal-based direct reduction processes, the recovery rates of titanium, vanadium, and chromium are still low. In addition, it should be noted that it is difficult to deal with BF slag while the coal-based direct reduction process has a relatively low efficiency due to its high energy consumption and high operating temperature [3–5]. None of the above techniques can be easily implemented in industrial production and commercial use, hindering the development of sustainable metallurgy.

Therefore, for efficient HVTM utilization, a novel and sustainable smelting process has been proposed by our laboratory that obtains a significant increase in the recovery rates of valuable elements. In this process, HVTMs were first pelletized and oxidized by roasting (HVTMP) and then were reduced in a shaft furnace. Subsequently, the reduced HVTMPs were separated by melting for the comprehensive recovery of iron, titanium, vanadium, and chromium [6]. It is clear that the melting separation is an essential procedure in this novel and sustainable smelting process. It is known that in the melting separation process, the fluidity of the titanium slag at high temperature can affect the separation of iron and slag, thus, affecting the efficiency of the subsequent titanium extraction. Moreover, the extraction efficiency is closely related to the mineral composition and the microstructure of the slag which depend on the chemical composition, initial melting state, and cooling conditions. Therefore, to achieve high extraction efficiency of titanium, it is necessary to improve the fluidity of the slag.

In the melting separation process, CaF_2 and B_2O_3 are commonly used as additives due to their remarkable effect on the fluidity of the slag. CaF_2 breaks up into small particles at high temperature and then melts quickly, decreasing the melting temperature and viscosity of slag. Although CaF_2 plays an important role in the metallurgical industry, its use leads to significant environmental pollution that is inconsistent with the development of sustainable metallurgy [7–10]. In the past decades, many studies have proposed to replace CaF_2 with B_2O_3 that not only avoids the disadvantages of CaF_2 but also achieves a better metallurgical effect than CaF_2. The acidity of B_2O_3 is clearly stronger than that of SiO_2. Therefore, the CaO in the slag reacts preferentially with B_2O_3 to form $nCaO{\cdot}B_2O_3$ with a low melting point and then promotes the melting of lime. At the same time, the slag viscosity decreases with increasing B_2O_3 content. This improves the diffusion and mass transfer in the melting separation process, which is beneficial for the slag system and the melting separation process [9, 11–18].

The melting temperature and viscosity are crucial physical properties for the fluidity of slag. The effect of B_2O_3 on the slag properties has been examined in previous studies [19–25]. Wang et al. investigated the influence of B_2O_3 on the melting temperature and viscosity of refining flux. It was demonstrated that B_2O_3 was beneficial for decreasing the melting temperature and viscosity [20]. Ren et al. investigated the effect of B_2O_3 on the viscosity of Ti-bearing blast furnace slag and showed that the addition of B_2O_3 decreased the viscosity and improved the fluidity of the slag [21]. Li et al. found that for the $CaO–SiO_2–Al_2O_3–Cr_2O_3$ slag, B_2O_3 behaved as a network former to decrease the number of non-bridging oxygen atoms per Si atom (NBO/Si). Unfortunately, the addition of B_2O_3 also resulted in the formation of low-melting-point eutectics and decreased the structural strength of the obtained metal [23]. To summarize, the studies performed to date have mainly focused on the effect of B_2O_3 on the blast furnace slag, mold flux, or refining slag. However, there have been few reports on the effect of B_2O_3 on the properties of high-titanium melting slag, particularly in the presence of chromium. In the Cr-containing high-titanium melting slag ($CaO–SiO_2–MgO–Al_2O_3–TiO_2–Cr_2O_3$), the TiO_2 content is higher than that in the Ti-bearing blast furnace slag, and considerable utilization can be obtained if the titanium can be extracted effectively. Therefore, it is urgently necessary to improve the fluidity of the Cr-containing high-titanium melting slag.

In this study, B_2O_3 was introduced as a fluxing agent into the Cr-containing high-titanium melting slag, and the effect of B_2O_3 on the melting temperature and viscosity of this slag was investigated. In particular, the evolution of the phase composition and structure was examined. This study provides reference data for an environmental-friendly metallurgical process and also provides the basis for the subsequent extraction of titanium and other valuable elements. Thus, this work contributes to the development of sustainable metallurgy.

Experimental

Sample Preparation

To ensure the accuracy of the experiments, the samples were pre-melted to form a homogeneous slag. Certain amounts of oxides (Table 1) were proportionally weighed, mixed, and placed into a graphite crucible lined with molybdenum flakes and then were placed in a $MoSi_2$ resistance furnace. The mixture was melted under argon atmosphere at 1550 °C. After full stirring, the slag was removed, cooled, and crushed for further experiments.

Experimental Apparatus

Figure 1 shows a schematic diagram of the instrument used for melting-point and melting-rate measurements that consists of three components, namely a light source, a heat

Table 1 Chemical composition of Cr-containing high-titanium melting slag (wt%)

No	CaO	SiO_2	MgO	Al_2O_3	TiO_2	Cr_2O_3	B_2O_3
1	14.71	21.02	11.22	10.42	40.63	2.00	0.00
2	14.30	20.43	11.22	10.42	40.63	2.00	1.00
3	13.89	19.84	11.22	10.42	40.63	2.00	2.00
4	13.48	19.25	11.22	10.42	40.63	2.00	3.00
5	13.07	18.66	11.22	10.42	40.63	2.00	4.00

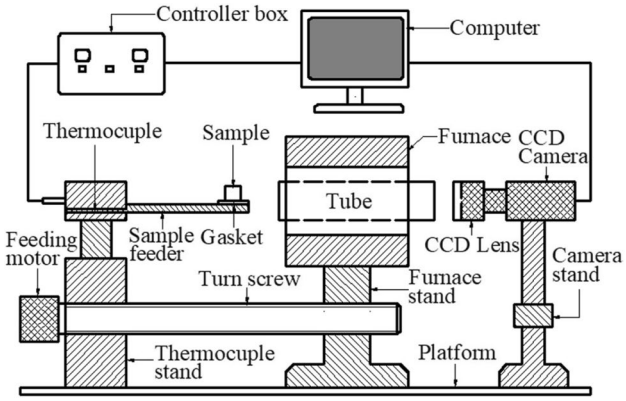

Fig. 1 Schematic diagram of the experimental apparatus for melting temperature

source (an electric furnace with an alumina tube), and a camera system. A U-shaped $MoSi_2$ is used as the heating element, and the highest operating temperature is 1550 °C. The temperature control precision is ± 2 °C and the heating thermocouple is located at the bottom of the sample and can display the temperature change. To reduce the experimental error, two sets of temperature readings were obtained for the same sample. If the difference between the two readings exceeded 3 °C, the sample was tested again.

The viscosity was measured using an RTW-10 melting physical property comprehensive measurement instrument designed by Northeastern University, as shown in Fig. 2. This system enables the continuous measurement of the viscosity during the cooling process and the fixed-point measurement of the viscosity at a constant temperature. The heating element consists of a U-shaped $MoSi_2$ and a Pt–Rh thermocouple to ensure that the temperature deviation in the constant zone is less than 1 °C. The spindle is made of molybdenum and the connecting rod is made of corundum.

Experimental Procedure

The slag was ground to 74 μm in an agate mortar and the standard sample was prepared by pressing the slag into the cylinder. Then, the standard sample was placed on a corundum sheet in the middle of the tube. The shape change of the standard sample was observed and the melting behavior was described by three characteristic temperatures. When the height of the standard sample decreased one fourth of its original height, the corresponding temperature was recorded as the softening temperature (ST). The hemispherical temperature (HT) was the temperature at which the height of the standard sample decreased to one half of its original height. In addition, this temperature was defined as the melting temperature and this method of temperature measurements is called the hemispherical method [25]. The flow temperature (FT) was the temperature at which the sample was liquefied and its height decreased three fourths of its original height. Figure 3 shows the morphology and characteristic temperature of the standard samples with different B_2O_3 contents in the heating process.

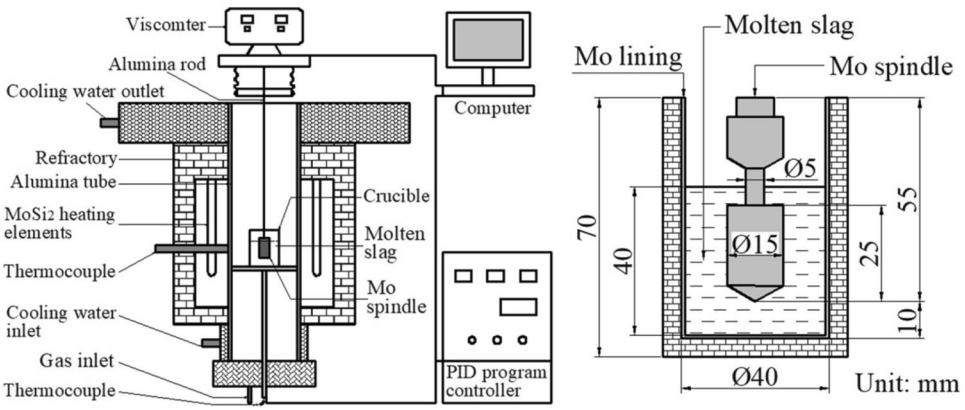

Fig. 2 Schematic diagram of viscosity furnace and detailed crucible size

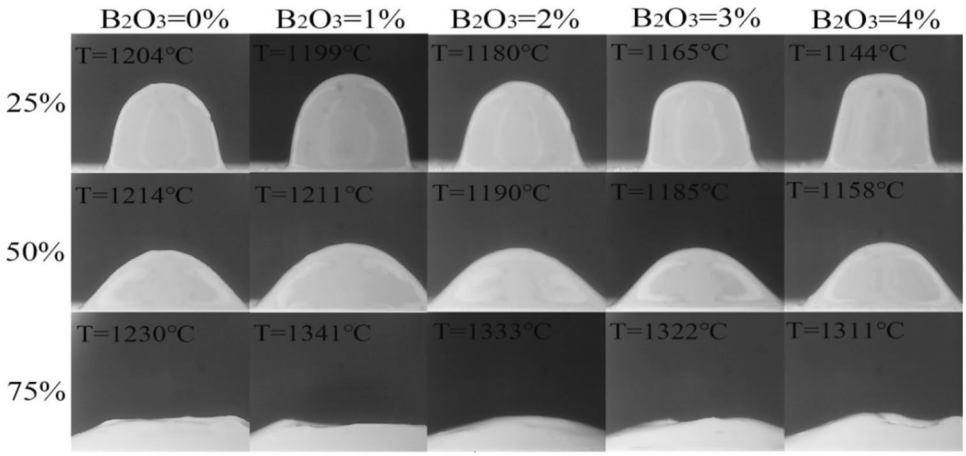

Fig. 3 Morphology and characteristic temperature of standard sample with different B_2O_3 contents

Prior to carrying out the viscosity experiment, the viscometer was calibrated using castor oil at room temperature [26–28]. The distance between the spindle and the bottom of the crucible was maintained at 10 mm. When the furnace temperature reached 1550 °C, the slag was kept at this temperature for 1 h, and then the viscosity measurement was carried out as the temperature decreased. To avoid the measurement interruption caused by the overload of the torque sensor, the viscosity measurement was terminated immediately when the viscosity reached 5 Pa s. During the viscosity measurement, the slag was fully liquid and acted as a Newtonian fluid. Each experiment was conducted twice to ensure the reliability of the results. Argon was used as the protective gas throughout the experiment.

When the viscosity measurement was completed, the furnace temperature decreased to 1100 °C, and the slag solidified. Then, the slag was removed from the furnace and was air cooled to room temperature. The slag sample was broken, and a uniform size was selected. To obtain a smooth surface, the sample was first polished using sand paper with different roughness grades from coarse to fine and then polished using a polishing machine. To improve its electrical conductivity, gold was sprayed onto the detection surface prior to scanning electron microscopy (SEM) observation. The other part was ground in an agate mortar and then filtered by a 200-mesh filter sieve. Then, the obtained powder was used for X-ray diffraction (XRD) analysis.

Characterization

The composition of the precipitated phase was identified by XRD (PANalytical) using Cu-Kα radiation with the voltage and current of 40 kV and 40 mA, respectively. The morphology of the precipitated phase was observed by SEM (Ultra Plus; Carl Zeiss GmbH, Jena, Germany) with energy dispersive spectroscopy (EDS) using a Schottky-type field emission electron source and resolution ratios of 0.8 nm/15 kV and 1.6 nm/1 kV at 20 V to 30 kV.

Results and Discussion

Effect of B_2O_3 on the Melting Property

The results of the effect of B_2O_3 on the characteristic temperature of Cr-containing high-titanium melting slag are shown in Fig. 4. With the increase of B_2O_3 content from 0 to 4%, the ST and the HT clearly decreased from 1204 and 1214 °C to 1144 and 1158 °C, respectively. It should be noted that the FT of the slag with B_2O_3 was higher than that without B_2O_3, which may be due to the expansion of the slag after the addition of B_2O_3. This gives rise to a severe flow deformation. On one hand, it is well known that B_2O_3 is an acid oxide. When B_2O_3 was added to the slag, according to ionic theory, the anionic structure became complicated, and the electrostatic attraction acting on the cations decreased,

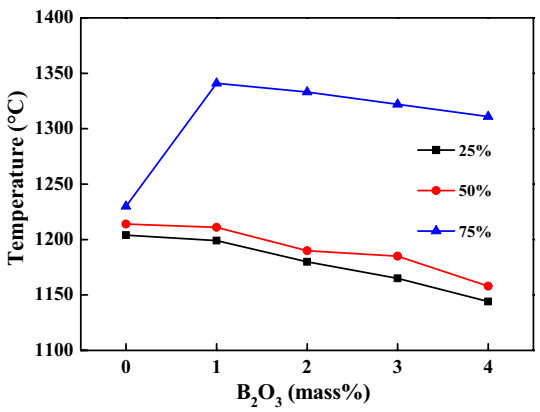

Fig. 4 Characteristic temperature of Cr-containing high-titanium melting slag with different B_2O_3 contents

decreasing the surface tension. Therefore, the volume of the slag increased. On the other hand, at higher temperature, when B_2O_3 was not added, the fluidity of the slag is poor due to its complex structure. However, when B_2O_3 was added, it gave rise to a "flooding phenomenon" and increased the volume of the slag. The volume and height of the slag decreased only after the "bubble" was broken. Therefore, the flow temperature of the slag with B_2O_3 was higher than that without B_2O_3. When the temperature reached FT, the slag melted. However, when B_2O_3 content increased from 1 to 4%, the FT decreased.

Since B_2O_3 is a typical acid oxide with a low melting point (~ 450 °C) [29], the presence of B_2O_3 is conducive to the fusing of CaO, Al_2O_3, and other high-melting-point components into slag and decreases the melting point of the slag. Additionally, B_2O_3 can easily combine with various oxides, forming low-melting-point eutectic crystals such as $MgO{\cdot}B_2O_3$ (988 °C) and $CaO{\cdot}B_2O_3$ (1100 °C). This is also conducive to the decrease of the melting temperature of the slag.

Effect of B_2O_3 on the Viscosity

Figure 5 shows the viscosity of the Cr-containing high-titanium melting slag with different B_2O_3 contents. It is clear that the viscosity increased with decreasing temperature. Another important finding was that the viscosity decreased significantly with the increase of B_2O_3 content, and this trend became more pronounced with higher B_2O_3 content. Generally, in a certain range of B_2O_3 content, a slag with high fluidity can be obtained at high temperature and high B_2O_3 content.

According to a previous study, B_2O_3 is an acid oxide and acts as a network former [30]. In the slag, boron is found in the form of $[BO4]^{5-}$ that gives rise to a more complex structure of the silicate network. This increases the degree of polymerization (DOP) and decreases the NBO/Si [31–38]. While the presence of B_2O_3 generally leads to the increase of slag viscosity, the opposite tend was observed for the high-titanium melting slag. This unusual behavior can be explained as follows. First, B–O bond is weaker than Si–O bond and breaks more easily, reducing the polymerization strength [17]. Second, although boron forms $[BO4]^{5-}$ with a complex network structure, the increase in the content of this structure is equivalent to the dilution of the complex silicate network structure [18, 39, 40]. Finally, B_2O_3 has a low melting point and can easily combine with many different oxides to form a low-eutectic mixture. This not only decreases the slag viscosity but also significantly decreases the melting temperature and finally improves the slag fluidity [15, 16, 29].

Crystallization Morphology

The crystallization morphology of the Cr-containing high-titanium melting slag with different B_2O_3 contents are shown in Fig. 6. It was observed that with increasing B_2O_3 content, the morphology and size of the precipitated phases presented dense and sparse distribution. When B_2O_3 was not added, two types of precipitated phases could be found, namely dark-gray matrix phase and light-gray phase. The EDS results show that the matrix phase and the light-gray long-stripe phase were silicate and titanium bearing, respectively. For the B_2O_3 content of 1%, the light gray phase was almost entirely found in the form of small particles and the long-stripe phase disappeared. The EDS results presented in Fig. 6g indicated that some boron-containing phases precipitated and the dark gray phase was still the silicate matrix.

When the B_2O_3 content increased to 2%, the small light-gray phase gradually grew to long stripe and almost disappeared. However, when the B_2O_3 content reached 3%, some new boron-containing phase precipitated. Moreover, based

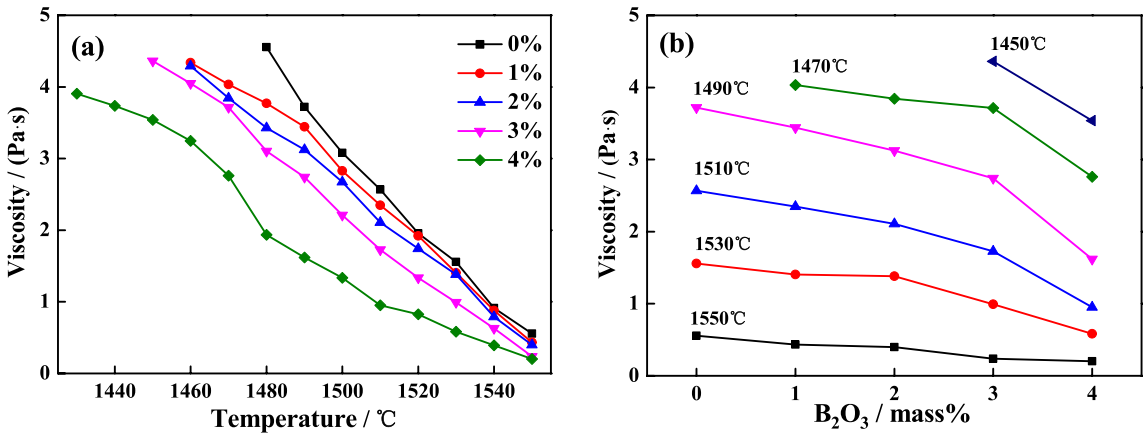

Fig. 5 Change of the viscosity of Cr-containing high-titanium melting slag with different B_2O_3 contents

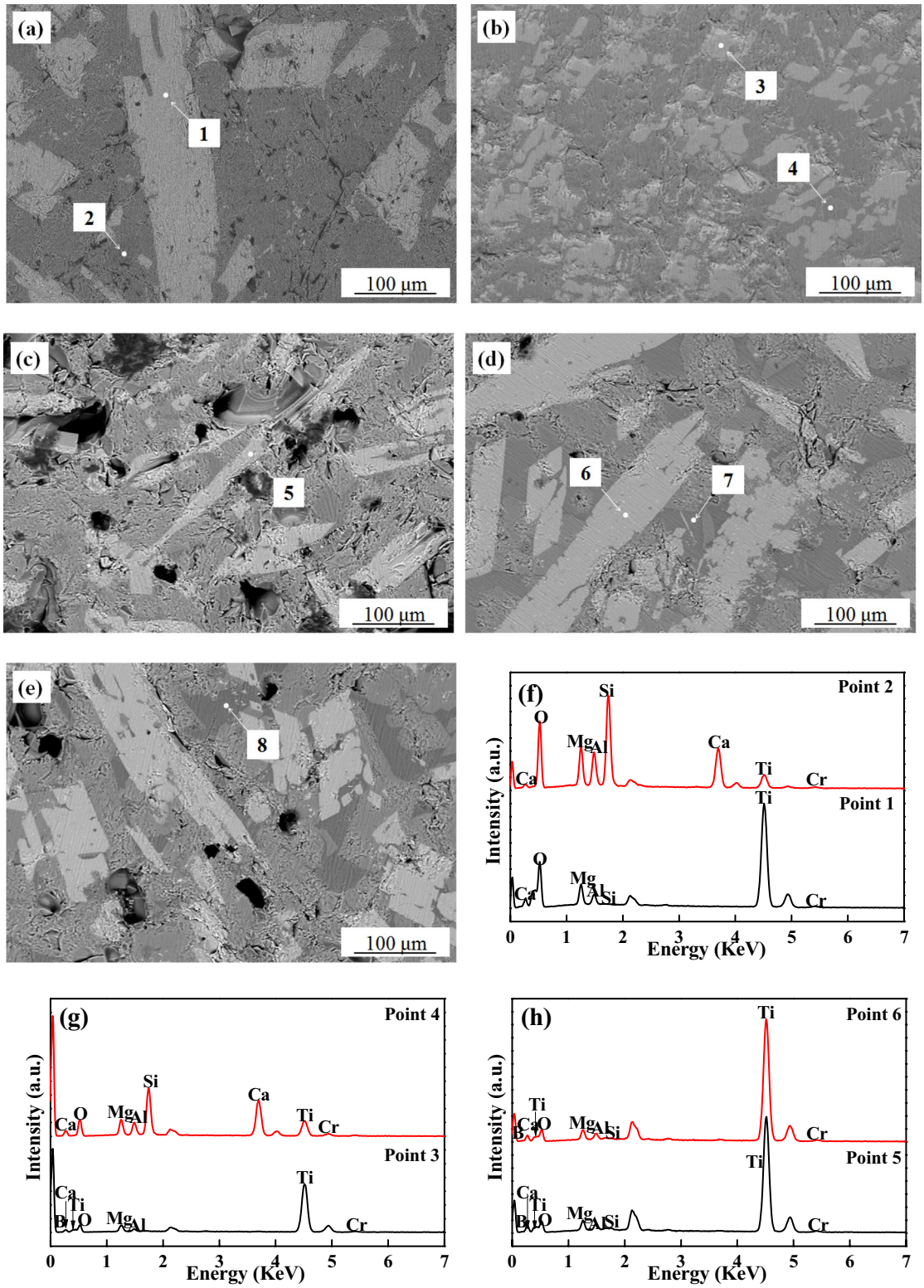

Fig. 6 SEM–EDS analysis of Cr-containing high-titanium melting slag with different B_2O_3 contents. **a** 0%, **b** 1%, **c** 2%, **d** 3%, **e** 4%, and **f–i** EDS analysis

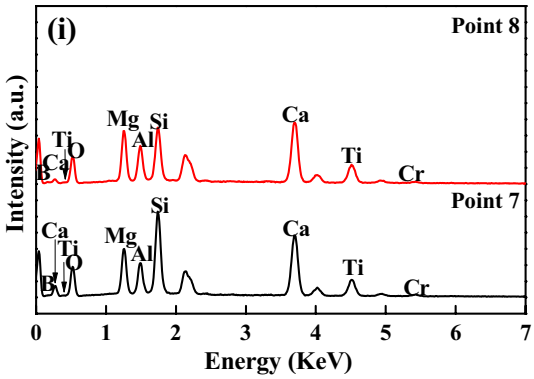

Fig. 6 (continued)

on the EDS results, it was determined that the new precipitated phase was borate. To determine the elemental distribution, EDS surface scanning was carried out, and the results are shown in Fig. 7. It was observed that Ca, Si, and Al were mainly concentrated in the matrix phase, while Ti was mainly concentrated in the long-stripe phase, and the other elements were evenly distributed. When the B_2O_3 content was 4%, the morphology and elemental composition did not change significantly, but the diffraction peak intensity of the precipitated borate phase increased.

Crystallization Phase Composition

The crystallization phase composition of the Cr-containing high-titanium melting slag was identified by XRD, and the results are shown in Fig. 8. In the absence of B_2O_3, six precipitated phases were found, namely anosovite ($MgTi_2O_5$), sphene ($CaTiSiO_5$), pyroxene ($CaMgSi_2O_6$, $CaTiSi_2O_6$), perovskite ($CaTiO_3$), anorthite ($CaAl_2Si_2O_8$), and spinel ($MgAlCrO_4$, $MgCr_2O_4$). After 1% B_2O_3 was added, the final precipitated phases contained several boron-containing phases such as kotoite ($Mg_3B_2O_6$), suanite ($Mg_2B_2O_5$), clinokurchatovite ($CaMgB_2O_5$), sinhalite ($MgAlBO_4$), warwickite ($MgTiBO_4$), and danburite ($CaB_2Si_2O_8$). When B_2O_3 content increased to 4%, the types of the precipitated phase did not change significantly, but the diffraction peak intensities did change. The spinel phase disappeared completely, and the diffraction peak intensity of the perovskite with a high melting point also decreased. Moreover, based on the diffraction peak intensities, danburite became the main phase, verifying the reliability of the SEM results.

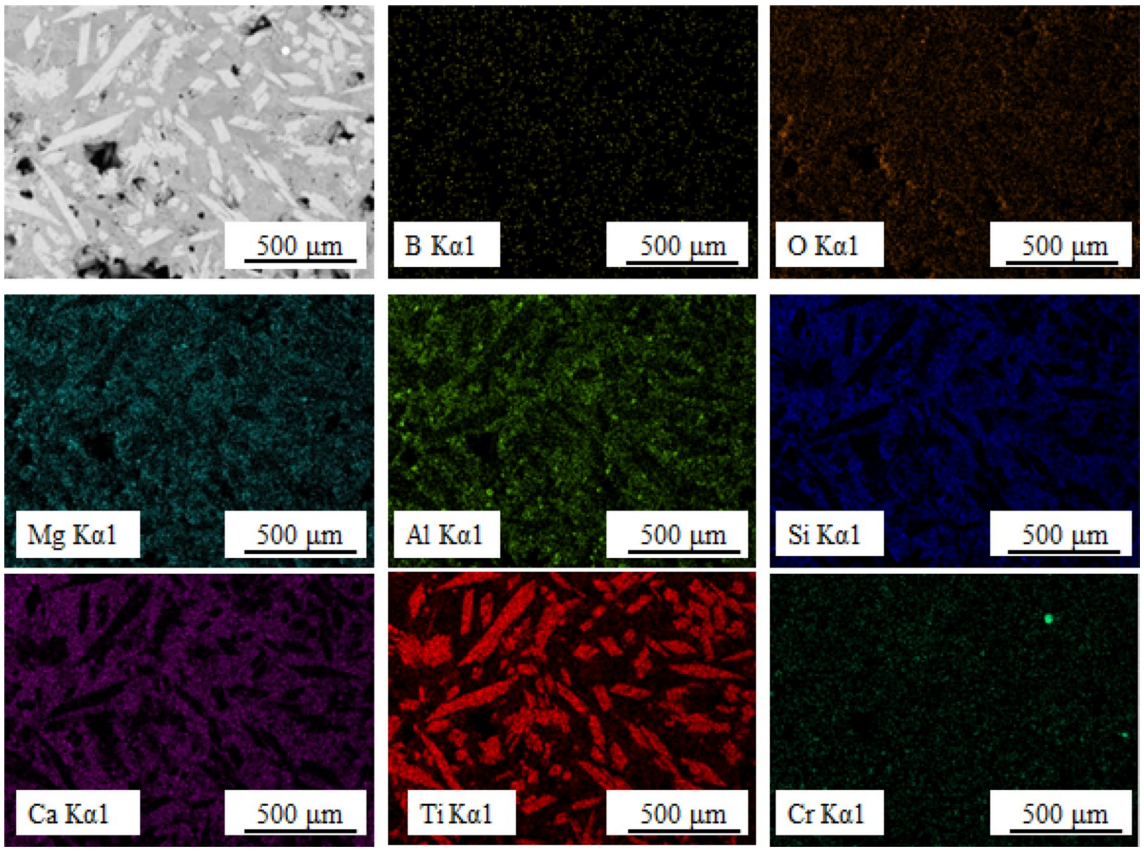

Fig. 7 Surface scanning of Cr-containing high-titanium melting slag with 3% B_2O_3

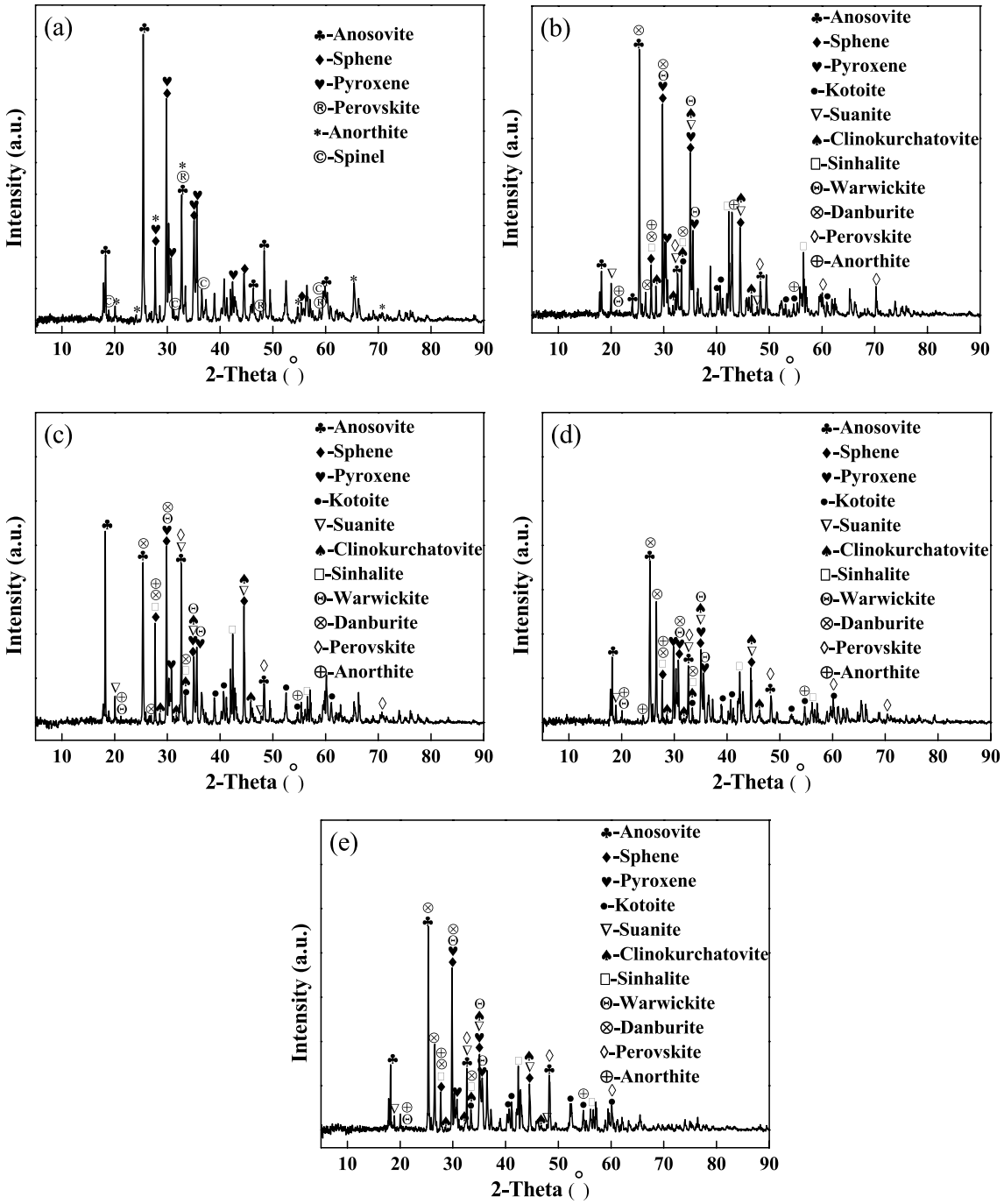

Fig. 8 XRD patterns of precipitated phases with different B_2O_3 contents. **a** 0%, **b** 1%, **c** 2%, **d** 3%, and **e** 4%

Discussion

Enrichment and extraction of titanium are important for the utilization of the Cr-containing high-titanium melting slag. However, the viscosity of the slag will increase due to the presence of chromium and this may greatly increase the difficulty of titanium extraction. Therefore, to improve the fluidity of the slag, B_2O_3 was introduced into the Cr-containing high-titanium melting slag. As different components have different effects on the slag system due to their different internal structures. Therefore, the elucidation of the relationship between the slag composition and its properties is a key goal of our investigations. Both the phase composition and microstructure of the slag directly reflect the internal structure and affected the melting and viscous properties of the slag. According to our experimental results, when the B_2O_3

content increased from 1 to 4%, the melting temperature decreased significantly. In addition, the viscosity of the slag gradually decreased with the increase in the temperature and the B_2O_3 content. This can greatly improve the fluidity of the slag, facilitate the separation of slag and iron, and decrease the iron loss. Moreover, the method of titanium enrichment plays a key role in the extraction of titanium.

As an acid oxide, B_2O_3 acts as a network former but still improves the fluidity of the slag at high temperature. B_2O_3 easily combined with other oxides to form low-melting-point eutectics, which was more effective in reducing slag viscosity. Addition of B_2O_3 depolymerized the complex 3-D $[BO_4]^{5-}$ into a simple 2-D $[BO_3]^{3-}$ structure, meanwhile, the bridging oxygen O^0 transformed into non-bridging oxygen O^- during depolymerization, depolymerizing the chain/molecule of the slag. These changes led to a decrease in the viscosity [41]. In addition, according to previous studies, the addition of B_2O_3 reduced the activation energy E_A [42, 43]. The decrease of E_A indicated that the $(BO_3)^{3-}$ of the planar triangle was the main boron-containing unit in the melt that was looser than that of (BO_4^{5-}) of the tetrahedral structure, implying that the addition of B_2O_3 was beneficial for improving the fluidity of slag [44]. In the absence of B_2O_3, the main enrichment phase of titanium was anosovite. However, after the addition of B_2O_3, the amount of the precipitated perovskite decreased and the titanium-bearing phase was mainly concentrated in anosovite, which was conducive for the subsequent titanium extraction process.

Conclusion

In this study, the effect of B_2O_3 on the melting temperature and viscosity of $CaO–SiO_2–MgO–Al_2O_3–TiO_2–Cr_2O_3$ slag was studied. The following conclusions were drawn:

(1) The addition of B_2O_3 is beneficial for decreasing the melting temperature. When the B_2O_3 content increased from 0 to 4%, the melting temperature decreased from 1214 to 1158 °C. In addition, the softening temperature and the flow temperature also decreased by 60 °C and 30 °C, respectively.

(2) The viscosity decreased with increasing B_2O_3 content, particularly when the B_2O_3 content increased from 3 to 4%. Thus, an increase of B_2O_3 content in a certain range greatly improves the fluidity of the slag.

(3) B_2O_3 had a strong effect on the morphology of the precipitated phase as manifested in the size and shape of the precipitate particles. The morphology of the precipitated phase changed from small sheets to long stripes. In addition, the increase in the B_2O_3 content led to anosovite and danburite becoming the main precipitated phases and inhibited the precipitation of perovskite, which was beneficial for the subsequent titanium extraction process.

4) The addition of B_2O_3 to $CaO–SiO_2–MgO–Al_2O_3–TiO_2–Cr_2O_3$ slag is highly great significant for the improvement of slag fluidity and environmentally friendly, as well as for the development of sustainable metallurgy.

Acknowledgements This work is financially supported by the National Natural Science Foundation of China (Grant No. 51904066), Liaoning Revitalization Talents Program (Grant No. XLYC1802032), Fundamental Research Funds for the Central Universities (Grant No. N182503032), Postdoctoral Foundation of Northeastern University (Grant No. 20190201), and Postdoctoral International Exchange Program (Dispatch Project, 20190075).

Declarations

Conflict of interest On behalf of all authors, the corresponding author states that there is no conflict of interest.

References

1. Hu T, Lv XW, Bai CG, Lun ZG, Qiu GB (2013) Carbothermic reduction of titanomagnetite concentrates with ferrosilicon addition. ISIJ Int 53:557–563
2. Lv XW, Lun ZG, Yin JQ, Bai CG (2013) Carbothermic reduction of vanadium titanomagnetite by microwave irradiation and smelting behavior. ISIJ Int 53:1115–1119
3. Shi LY, Zhen YL, Chen DS, Wang LN, Qi T (2018) Carbothermic reduction of vanadium-titanium magnetite in molten NaOH. ISIJ Int 58:627–632
4. Long HM, Chun TJ, Wang P, Meng QM, Di ZX, Li JX (2016) Grinding kinetics of vanadium-titanium magnetite concentrate in a damp mill and its properties. Metall Mater Trans B 47:1765–1772
5. Wang YZ, Zhang JL, Liu ZJ, Du CB (2017) Carbothermic reduction reactions at the metal-slag interface in Ti-bearing slag from a blast furnace. JOM 69:2397–2403
6. Li W, Fu GQ, Chu MS, Zhu MY (2017) Gas-based direct reduction of Hongge vanadium titanomagnetite-oxidized pellet and melting separation of the reduced pellet. Steel Res Int 88:1–10
7. Samal S, Mohapatra BK, Mukherjee PS (2010) The effect of heat treatment on titania slag. J Min Met Charact Eng 9:795–809
8. Chen G, Chen J, Song ZK, Srinivasakannan C, Peng JH (2014) A new highly efficient method for the synthesis of rutile TiO_2. J Alloys Compd 585:75–77
9. Fox AB, Mills KC, Lever D, Bezerra C, Valadares C, Unamuno I, Laraudogoitia JJ, Gisby J (2005) Development of fluoride-free fluxes for billet casting. ISIJ Int 45:1051–1058
10. Klug JL, Silva DR, Freitas SL, Pereira MMSM, Heck NC, Vilela ACF, Jung D (2012) Fluorine-free mould powders for billet casting-technological parameters and industrial tests. Steel Res Int 83:791–799
11. Mills KC, Fox AB, Li Z, Thackray RP (2005) Performance and properties of mould fluxes. Ironmak Steelmak 32:26–34
12. Zhou LJ, Wang WL, Wei J, Lu BX (2013) Effect of Na_2O and B_2O_3 on heat transfer behavior of low fluorine mold flux for casting medium carbon steels. ISIJ Int 53:665–672
13. Qi X, Wen G, Tang P (2008) Investigation on heat transfer performance of fluoride-free and titanium-bearing mold fluxes. J Non-Cryst Solids 354:5444–5452

14. Viswanathan NN, Ji FZ, Sichen D, Seetharaman S (2001) Viscosity measurements on some fayalite slags. ISIJ Int 41:722–727
15. Wang HM, Yang LL, Zhu H, Yan YQ (2011) Comparison of effects of B_2O_3 and CaF_2 on metallurgical properties of high basicity CaO-based flux. Adv Mater Res 311:966–969
16. Qi X, Wen GH, Tang P (2010) Viscosity and viscosity estimate model of fluoride-free and titanium-bearing mold fluxes. J Iron Steel Res 17:6–10
17. Na XZ, Xue M, Zhang XZ, Gan Y (2007) Numerical simulation of heat transfer and deformation of initial shell in soft contact continuous casting mold under high frequency electromagnetic field. J Iron Steel Res Int 14:14–21
18. Li GR, Wang HM, Dai QX, Zhao YT, Li JS (2007) Effect of additives on melting point of last refining ladle slag. J Iron Steel Res Int 14:25–29
19. Gao YH, Bian LT, Liang ZY (2015) Influence of B_2O_3 and TiO_2 on viscosity of titanium-bearing blast furnace slag . Steel Res Int 86:386–390
20. Wang HM, Zhang TW, Zhu H, Li GR, Yan YQ, Wang JH (2011) Effect of B_2O_3 on melting temperature, viscosity and desulfurization capacity of CaO-based refining flux. ISIJ Int 51:702–706
21. Ren S, Zhang JL, Wu LS, Liu WJ, Bai YN, Xing XD, Su BX, Kong DW (2012) Influence of B_2O_3 on viscosity of high Ti-bearing blast furnace slag. ISIJ Int 52:984–991
22. He SP (2010) Research of low fluorine and fluorine free mold fluxes. Chongqing University, Chongqing, pp 45–60
23. Li QH, Yang SF, Zhang YL, An ZQ, Guo ZC (2017) Effects of MgO, Na_2O, and B_2O_3 on the viscosity and structure of Cr_2O_3-bearing CaO–SiO_2–Al_2O_3 slags. ISIJ Int 57:689–696
24. Kim GH, Sohn I (2014) Role of B_2O_3 on the viscosity and structure in the CaO–Al_2O_3–Na_2O-based system. Metall Mater Trans B 45:86–95
25. Wang HM, Li GR, Dai QX, Li B, Zhang XJ, Shi GM (2013) CAS-OB refining: slag modification with B_2O_3–CaO and CaF_2–CaO. Ironmak Steelmak 34:350–353
26. Chen M, Raghunath S, Zhao BJ (2013) Viscosity measurements of "FeO"-SiO_2 slag in equilibrium with metallic Fe. Metall Mater Trans B 44:506–515
27. Xu RZ, Zhang JL, Wang ZY, Jiao KX (2017) Influence of Cr_2O_3 and B_2O_3 on viscosity and structure of high alumina slag. Steel Res Int 88:1–7
28. Kim JR, Lee YS, Min DJ, Jung SM, Yi SH (2004) Influence of MgO and Al_2O_3 contents on viscosity of blast furnace type slags containing FeO. ISIJ Int 44:1291–1297
29. Wang Q, Chi J (1991) Study on the physical and chemical properties of E_2 steel continuous casting mold slag. Sichuan Metall. 3:40–46
30. Wang Z, Shu QF, Chou KC (2013) Viscosity of fluoride-free mold fluxes containing B_2O_3 and TiO_2. Steel Res Int 84:766–776
31. Suito HK, Inoue R (2002) Dissolution behavior and stabilization of fluorine in secondary refining slags. ISIJ Int 42:921–929
32. Lai FF, Yao W, Li JL (2020) Effect of B_2O_3 on structure of CaO–Al_2O_3–SiO_2–TiO_2–B_2O_3 glassy systems. ISIJ Int 60:1596–1601
33. Park JY, Kim GH, Kim JB, Park S, Sohn I (2016) Thermo-physical properties of B_2O_3-containing mold flux for high carbon steels in thin slab continuous casters: structure, viscosity, crystallization, and wettability. Metall Mater Trans B 47:2582–2594
34. Kline J, Tangstad M, Tranell G (2015) A Raman spectroscopic study of the structural modifications associated with the addition of calcium oxide and boron oxide to silica. Metall Mater Trans B 46:62–73
35. Kim Y, Morita K (2014) Relationship between molten oxide structure and thermal conductivity in the CaO–SiO_2–B_2O_3 system. ISIJ Int 54:2077–2083
36. Yang J, Zhang J, Sasaki Y, Ostrovski O, Zhang C, Cai D, Kashiwaya Y (2017) Effect of B_2O_3 on crystallization behavior, structure, and heat transfer of CaO–SiO_2–B_2O_3–Na_2O–TiO_2–Al_2O_3–MgO–Li_2O mold fluxes. Metall Mater Trans B 48:2077–2091
37. Wang Z, Shu QF, Chou KC (2011) Structure of CaO–B_2O_3–SiO_2–TiO_2 glasses: a Raman spectral study. ISIJ Int 51:1021–1027
38. Sun YG, Zhang ZT (2015) Structural roles of boron and silicon in the CaO–SiO_2–B_2O_3 glasses using FTIR, Raman, and NMR spectroscopy. Metall Mater Trans B 46:1549–1554
39. Li LX, Jia R (2010) Physical chemistry of silicate. Metallurgical Industry Press, Beijing, pp 133–144
40. Qi CL, Zhang JL, Shao JG, Lu WJ, Zhao ZX, Zhang XS (2011) Study of boronizing mechanism of high-alumina slag. Steel Res Int 82:1319–1324
41. Wang G, Wang JS, Xue QG (2018) Properties of boron-rich slag separated from boron-bearing iron concentrate. J Cent South Univ 25:783–794
42. Wang L, Cui YR, Yang J, Zhang C, Cai DX, Zhang JQ, Sasaki Y, Ostrovski O (2015) Melting properties and viscosity of SiO_2–CaO–Al_2O_3–B_2O_3 system. Steel Res Int 86:670–677
43. Huang XH, Liao JL, Zheng K, Hu HH, Wang FM, Zhang ZT (2014) Effect of B_2O_3 addition on viscosity of mould slag containing low silica content. Ironmak Steelmak 41:67–74
44. Padmaja G, Kistaiah P (2009) Infrared and Raman spectroscopic studies on alkali borate glasses: evidence of mixed alkali effect. J Phys Chem A 113:2397–2404

Authors and Affiliations

Jing Ma[1,2] · Wei Li[1,2] · Guiqin Fu[1,2] · Miaoyong Zhu[1,2]

[1] School of Metallurgy, Northeastern University, Shenyang 110819, China

[2] Key Laboratory for Ecological Metallurgy of Multimetallic Mineral (Ministry of Education), Northeastern University, Shenyang 110819, China